QCES EDAA Lab Report: Modelling Methane Emission from a Cambridgeshire Landfill with Gaussian Plume Techniques

Unique ID: 135826

Due: 13/12/2024

Abstract

This report attempts to constrain the emissive methane (CH_4) flux from Milton Landfill using a steady-state gaussian plume model to reconstruct emissions from methance concentration data recorded at Microsoft Research Cambridge (MRC) in June 2024. Our model neglects the advection time of CH_4 in favour of a steady-state statistical model which depends only on the wind vector and atmospheric stability which we can reconstruct from the MRC data. Using the EPA's ISC3 model's parameters, we find that the flux depends on whether we take the model to be a point, line or area source. It is likely that the point source is the most physical model as the concentration seems best reproduced from the onsite gas flaring plant's emissions, though the areal source provides a qualitiatively good fit at low concentrations. Other than three "spike" events, likely associated with landfill collapse or methane release events, the background flux is between 7.75 $g\,s^{-1}$ and 2.65 $g\,s^{-1}$.

1 Introduction

Alongside CO_2, methane (CH_4) emissions are a dominant contributor to anthropogenic warming and climate risk. Limiting human-caused warming requires a strong reduction in CH_4 emissions (IPCC 2023). Waste disposal emits the second most CH_4 of any sector in the EU, of which landfill emissions are the largest source (2.3% of total CO_2 equivalent) (EEA 2023). Globally, solid waste makes up 11% of CH_4 emissions (CCA 2022), and 24% of UK emissions (DESNZ 2024).

Landfill waste emissions reductions have been the primary force in the reduction of UK CH_4 emissions, but this may have stalled (ECCC 2024). Measuring these emissions is important to quantify their impact.

1.1 Motivation

There is not currently good quality, high-resolution, local-scale data on methane emissions from landfill sites. Landfill gas (LFG) emissions are generally estimated using gas generation models which often do not hold up to verification. (Mønster, Kjeldsen, and Scheutz 2019).

Temporal variability in LFG emissions is associated with changes in pressure (Kissas et al. 2022), precipitation (Delgado et al. 2022), wind speed, temperature, moisture, surface cracking and animal activity (Rachor et al. 2013). This provides difficulties in measuring a good range of data, so modelling plumes may allow us to get longer timescale results with a variety of atmospheric conditions. Dispersion modelling allows us to estimate emission from samplers outside the landfill, therefore we can leverage existing datasets to analyse emissions without further measurements.

In this report, we use a Gaussian plume model to estimate a landfill's methane emissions, and discuss the trends in flux. Specifically, whether modelling the source as a point, line or area is more appropriate. Additionally, we attempt to verify the relationships with precipitation and temperature predicted by Kissas et al. 2022, Delgado et al. 2022 and Rachor et al. 2013.

1.2 Study Area

Our area of interest spans from Milton Landfill, (52.246°N, 0.1436°E) to Microsoft Research in Cambridge Science Park (52.237111°N, 0.144343°E). Anglian Water Cambridge Water Recycling Center (CWRC), (52.2335 °N, 0.157 °E), likely also produces methane (Lyon 2012).

Milton Landfill occupies an area of 48.5 ha in 24 "cells", which are used and capped sequentially. Cells 1-14B were capped as of 2022, and all cells were to be completed by 2025. The site is shown in

Figure 3. Ages of cell burial likely provides a control on CH_4 emissions (T.H. Christensen and Stegmann 2020).

The site generates CH_4 and other landfill gases by anaerobic decomposition of organic waste. LFG is extracted by a system of wells and piped to an on-site gas plant. Excess gas is flared, which releases much more CH_4 than background emission. Liners on cells and progressive capping limit emissions. The LFG measured by FCC is 41.4% Methane (ByrneLooby 2022).

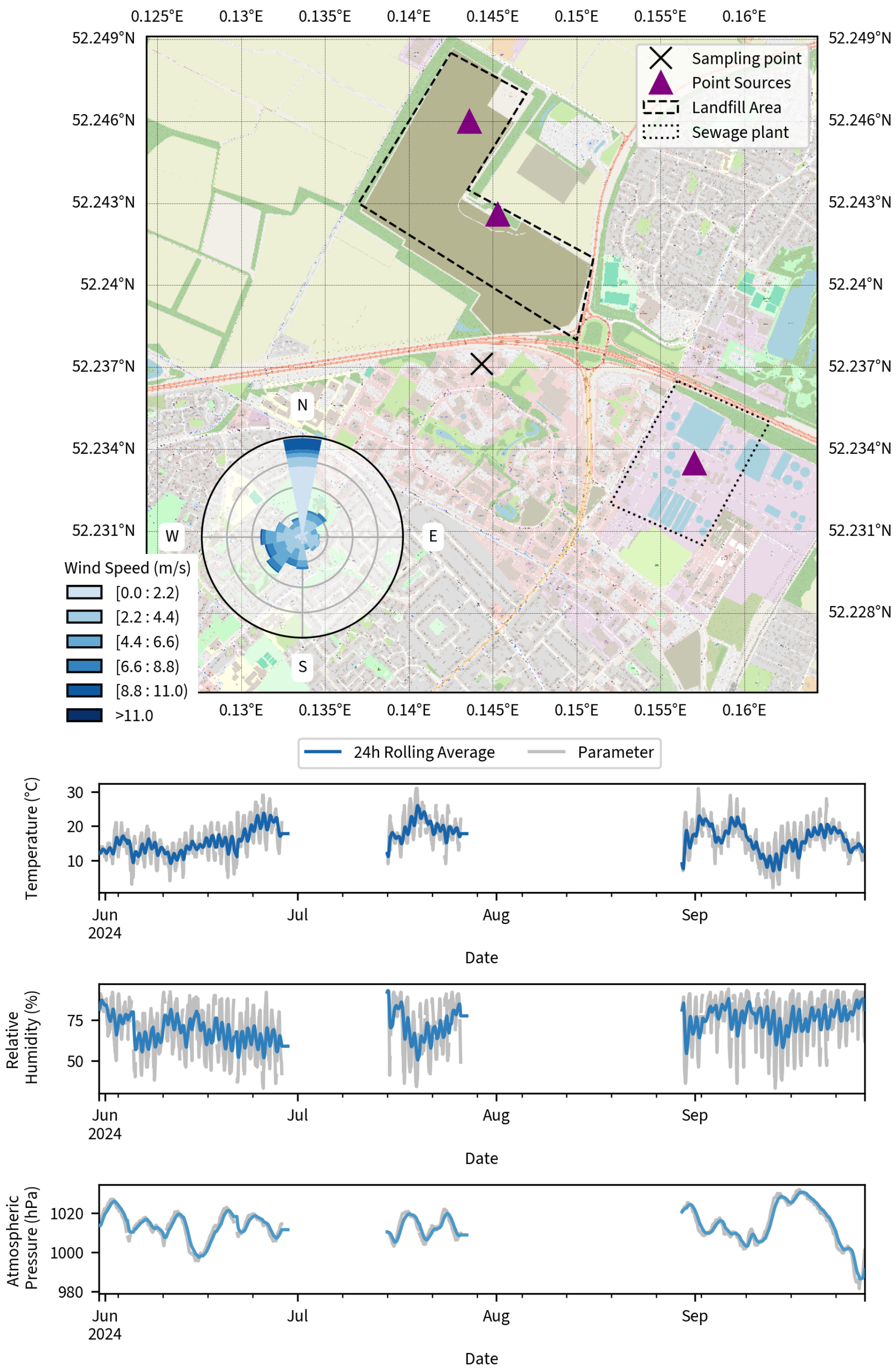

Figure 1: Map of the study area and meteorological overview. Note significant periods in July and August where no data is present.

1.3 Aims

- Use the provided dataset to explain methane concentration between June 2024 and October 2024.
- Create a number of gaussian plume models for a statistical view of sampled methane concentration.
- Invert the gaussian plume model to estimate methane source flux from our landfill site.
- Explain the time series for emissive source flux.

2 Methods

2.1 Dataset

The dataset consists of hourly measurements of methane concentrations from a sampler located at Cambridge Science Park, as well as co-located meteorological data: wind speed, wind direction, humitidy, and temperature. The dataset features two large breaks in recording. Some values required filtering, described in Appendix A. A representative row from the dataset is reproduced in table 1.

Date	ALTM_hPa	temp	DEW_C	rh	wd	ws	nsec	lat	lon
2024-05-31 13:00:00	1019.3	14	11	85	350	7	3926149200	52.42	0.57

altinmeters	nsec.licor	co2_ppm	h2o_ppm	ch4_ppb
10	3926149200	529.343981189144	13012.0577874091	2309.41718939563

ch4_ppm	latitude2	longitude2
2.30941718939563	52.237111	0.144343

Table 1: A representative row from the dataset. Data is taken from Fotherby 2024.

2.2 Model

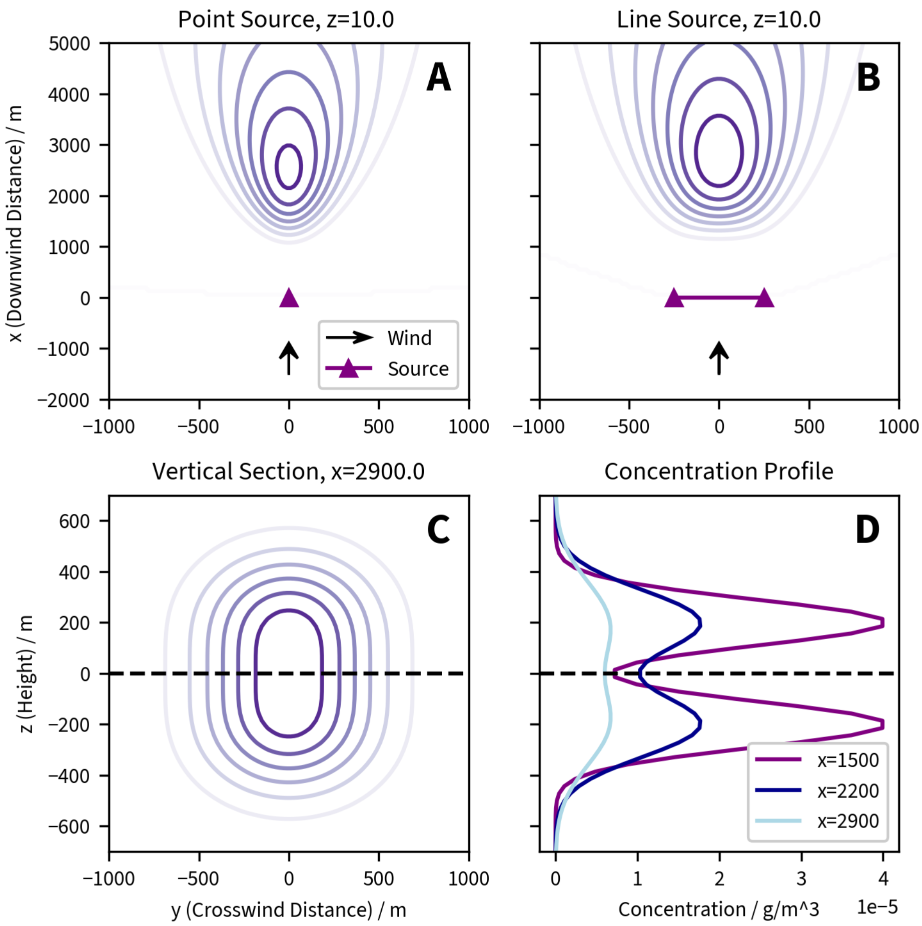

Figure 2: Simplified diagram of Gaussian plume dispersion with concentration contours plotted. σ_y and σ_z act in the the y and z directions respectively. Note that negative heights have been visualised to show the effect of the second (reflective) exponential term.

2.2.1 Gaussian Dispersion

The Gaussian dispersion equation is commonly used to estimate contribution of a source to a pollutants' concentration without modelling eddy turbulence and diffusion (Stockie 2011; Sutton 1947; Beychok 1994, p. 24; Manheim et al. 2023). It makes a number of assumptions:

- Advection is much faster than downwind diffusion.
- No crosswind advection.
- Timescale of changing wind direction is longer than advection.
- Advective transport by wind velocity is uniform in space.
- Diffusivity is isotropic and only changes in the downwind direction.
- All pollutants that reach the surface are reflected.
- Variations in topography are negligible.

Point Source

A Gaussian plume is an analytical solution for the advection diffusion equation (Stockie 2011). The equation for Gaussian dispersion from a point source is given by:

$$C(x,y,z) = \frac{Q}{u\sigma_z\sigma_y 2\pi} e^{-\frac{y^2}{2\sigma_y^2}} \left[e^{-\frac{(z_y-H_0)^2}{2\sigma_z^2}} - e^{-\frac{(z_y+H_0)^2}{2\sigma_z^2}} \right] \tag{1}$$

where

$Q \Rightarrow$ emissive flux at the point source. (kg/s)

$u \Rightarrow$ wind speed. (m/s)

$\sigma_y \Rightarrow$ standard deviationin the y-direction. (m)

$\sigma_z \Rightarrow$ standard deviation in the z-direction. (m)

$H_0 \Rightarrow$ effective height of the plume above the ground. (m)

$x, y, z \Rightarrow$ distances from the ground at the base of the plume source (downwind, crosswind, and vertical). (m)

The Standard Deviations are modelled by the ISC3 model using the Pasquill-Gifford (PG) stability (Pasquill 1961; SCRAM 1995):

$$\sigma_z = ax^b \tag{2}$$
$$\sigma_y = 465.11628x \tan\theta \tag{3}$$
$$\theta = 0.017453293(c - \ln d) \tag{4}$$

The values of a, b, c and d are empirically determined; Here taken from the EPA's ISC3 model. Parameters used are tabulated in Table 2 for varying PG classes.

Stability Class	a	b	c	d
A	170.0	1.09	24.0	2.5
B	98.0	0.98	18.0	1.8
C	61.0	0.91	12.0	1.1
D	32.0	0.81	8.0	0.72
E	21.0	0.75	6.0	0.54
F	14.0	0.68	4.0	0.36

Table 2: ISC3 model parameters for the standard deviations of the plume. (SCRAM 1995)

Given the gas collection at the landfill, a point source flux seems likely; we can estimate the location of the LFG emissions based on ByrneLooby 2022 and satellite imagery, shown in Figure 3. Additionally, the difference in elevation (source height) is 9m.

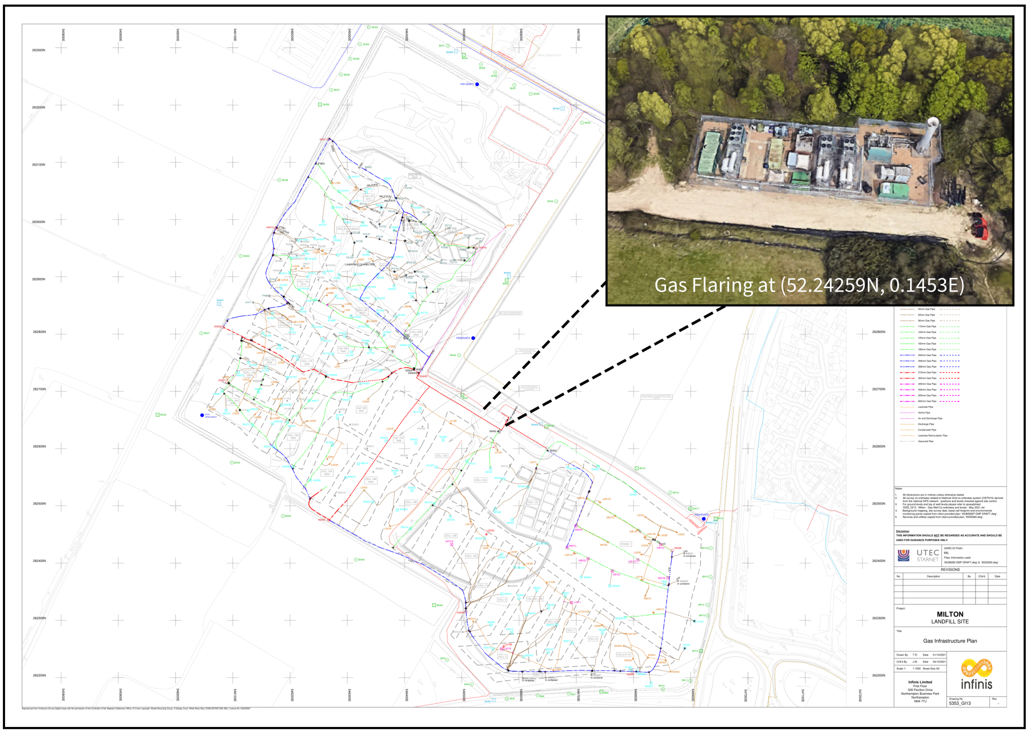

Figure 3: Image from Google Earth overlaid on map reproduced from ByrneLooby 2022 showing the location of the LFG plant, featuring three Jenbacher gas engines and a stack for gas flaring. Landfill cells are marked on the base map.

Line Source

For a line we can simply integrate the above function in y from $y - L/2$ to $y + L/2$, where L is the source width. We will also assume that the wind direction is perpendicular to the line source to simulate width. This is similar to Carney and Dodd 1989, with the re-introduction of reflection.

$$C(x, y, z) = \frac{Q_l}{u\sigma_z 2\sqrt{2\pi}} \left[e^{-\frac{(z_y - H_0)^2}{2\sigma_z^2}} - e^{-\frac{(z_y + H_0)^2}{2\sigma_z^2}} \right] \left[\text{erf}(\frac{y + L/2}{\sqrt{\sigma_y}}) - \text{erf}(\frac{y - L/2}{\sqrt{\sigma_y}}) \right] \tag{5}$$

Note that Q in this case is a rate per unit length, i.e. (kg $s^{-1}m^{-1}$).

Justification for using a line source over a point source comes from the observation that emission will be more dispersed across the width of the landfill. If the LFG collection is ineffective, this diffuse emission will be blown towards our sampler as if presenting a line segment cross section to the wind.

In our model we will therefore rotate the line source to face the wind. If we had a long thin source we could instead rotate the wind grid, but rotating the source if valid for an equant source. (Nagendra and Khare 2002).

Area Source

We could integrate the previous model in the x direction to get a rectangular area source. Unfortunately, due to the complex dependence on x, this integral is impossible without numerical techniques (Stockie 2011). Approximations by multiple line sources multiplied by small thicknesses approach the value of an areal source (Smith 1993, Carney and Dodd 1989). Their model involves n source widthstrips of δX. Their width L, is varied for each strip to model non-rectangular areas.

$$C(x, y, z) = \sum_{1}^{n} \frac{Q_a}{u\sigma_z\sigma_y 2\sqrt{2\pi}} \left[e^{-\frac{(z_y - H_0)^2}{2\sigma_z^2}} - e^{-\frac{(z_y + H_0)^2}{2\sigma_z^2}} \right] \left[\text{erf}(\frac{y + L/2}{\sqrt{\sigma_y}}) - \text{erf}(\frac{y - L/2}{\sqrt{\sigma_y}}) \right] \delta X \tag{6}$$

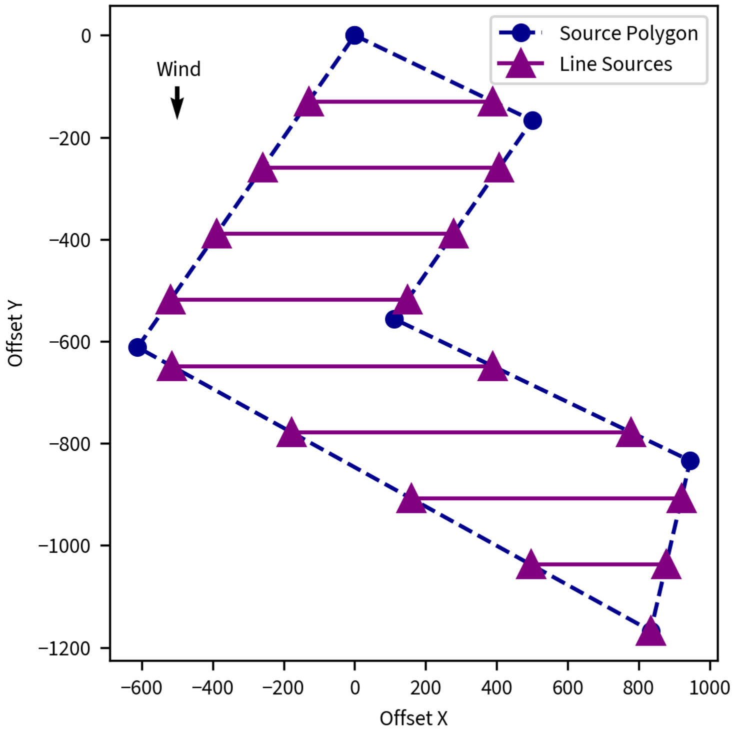

Figure 4: Geometry of a simulated areal source.

2.2.2 Estimating Source Flux

In order to invert the plume for source flux, we define the normalised concentration:

$$\Phi(x, y, z) = \frac{C(x, y, z)}{Q} \tag{7}$$

We divide our measured concentration by Φ to get the source flux Q. Additionally, we account for the atmospheric background as the C represents only the contribution due to the plume source. This was done by adding the minimum measured value (1978ppb) to C.

2.2.3 Model Assumptions

Our model makes assumptions further than those of the Gaussian plume model, and so the data is filtered. The main assumptions in this case are:

- The emissive flux at the source is constant (in section 3.2.1 only).
- The concentration is dominated by the landfill flux.
- The advection time is lower than our sampling rate.

We can estimate the constant emissive flux by using the average value of the emissions limits for permanent and temporarily capped cells (EA 2010). This gives a value of $Q = 0.01\,\mathrm{mg\,m^{-2}\,s^{-1}}$, or a total flux over the 48.5ha area of $Q = 4.85\,\mathrm{g\,s^{-1}}$.

To address the other assumptions, we perform two filtering steps on wind speed and direction, outlined in appendix A.

3 Results

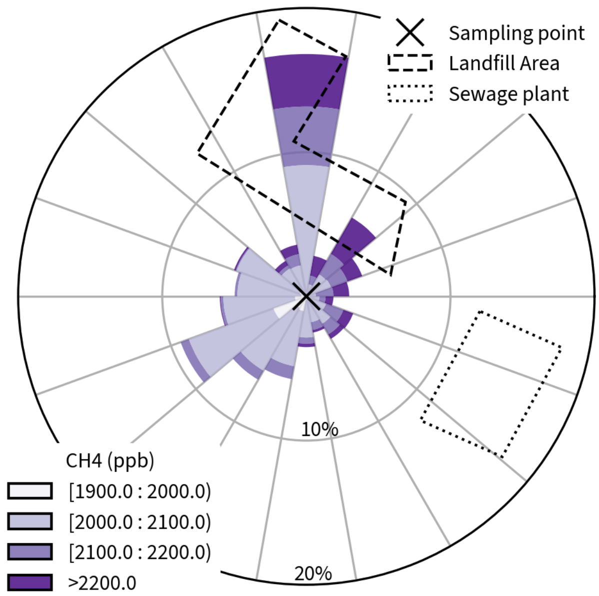

Figure 5: Methane concentrations from each wind direction measured at the MRC sampler as a fraction of time from June to October 2024.

3.1 Dataset

Figure 5 shows the predominant wind comes directly from the landfill site. High concentrations of methane are present for incoming wind bearings between (-10 and 110 degrees), dominantly from the landfill site, but some areas of high concentration when there is an Easterly wind may either be from the Water Recycling Plant or be due to a breakdown in the short timescale assumption for CH_4 transport (i.e. landfill CH_4 is being transported to the East and then blown back to our sampler by a Westerly wind).

Due to the relatively low frequency of Easterly winds, our assumption that the landfill dominates the concentration is likely true.

3.2 Model

3.2.1 Constant Flux Assumption

Beginning with a constant flux assumption and modelling forward for sampler concentration does not accurately produce a time series for concentration (Figure 6), but can inform our understanding of the source. Firstly, the point source located at the LFG treatment plant displays more similarity with the data than the point source at the centroid of the landfill. Additionally, when the magnitude of concentration is high, especially in late June, a point source at the location of the gas plant has more explanatory power. When the magnitude is low, such as in July, the area source produces a more accurate match to our measured data.

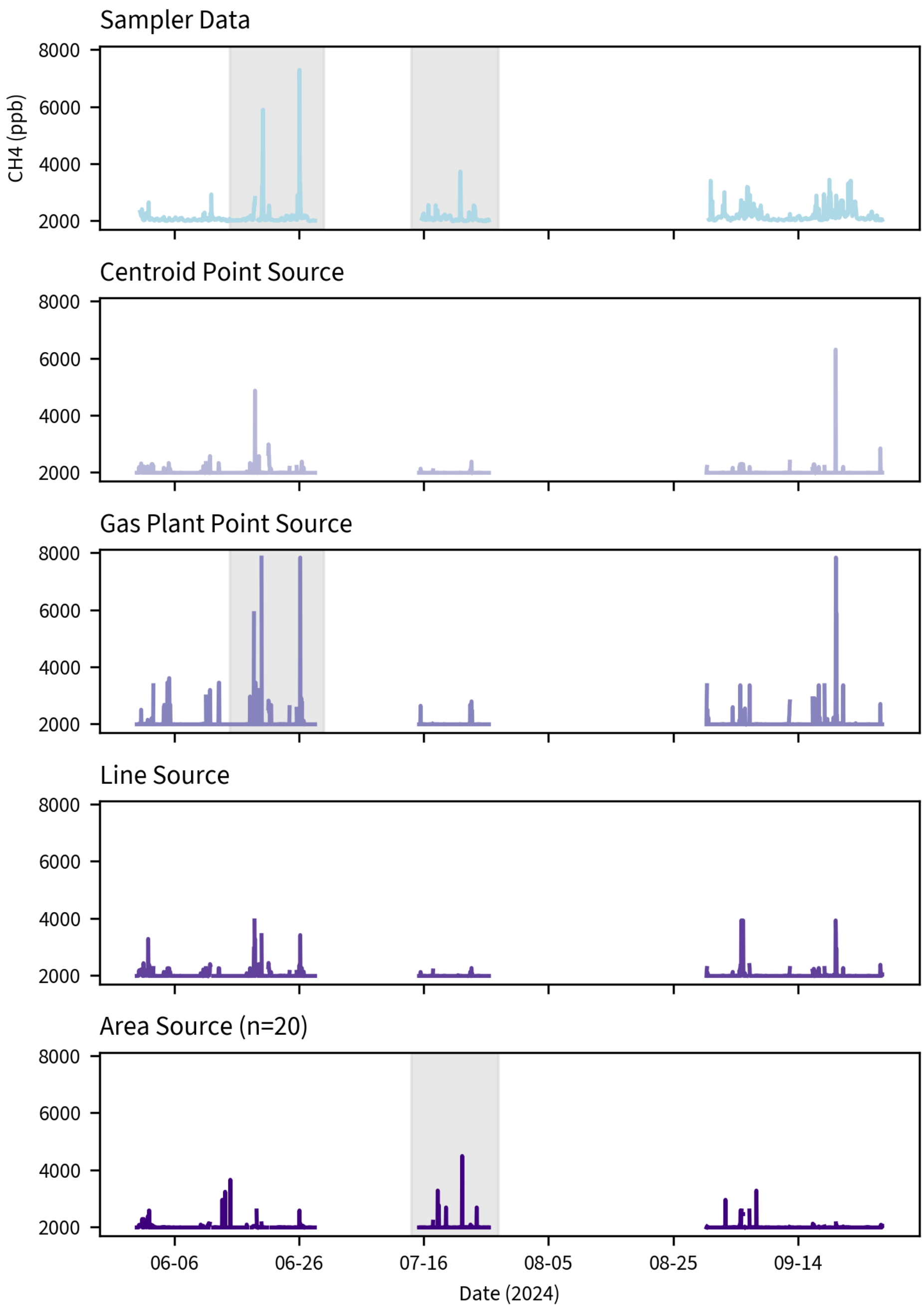

Figure 6: Constant flux model prediction for concentration based on weather data with three source geometries. Inset figure shows plume contours at marked time of high concentration.

3.2.2 Flux Estimation

Inverting the model using the method in section 2.2.2, we can reproduce a perfect fit to the data while the wind keeps the sampler close to directly downwind from the source. Outside of the that time, our assumption that the landfill dominates the CH_4 concentration breaks down. The differing lengths of lines in the area source results in inversion producing a range of unphysical values, therefore the use of area source for flux estimation was abandoned.

There is a good fit between the line and point source models in shape, but their magnitude differs, with the line source producing less total flux. The centroid model produced extreme values, which confirms that the LFG source is more likely.

In both models, there is a low background (approximately $10\,\mathrm{g\,s^{-1}}$) emission, which is interrupted by 3 large events. The average total emission is 7.75 g s^{-1} for the line source (after multiplying by the source width), and 2.65 g s^{-1} for the LFG plant point source.

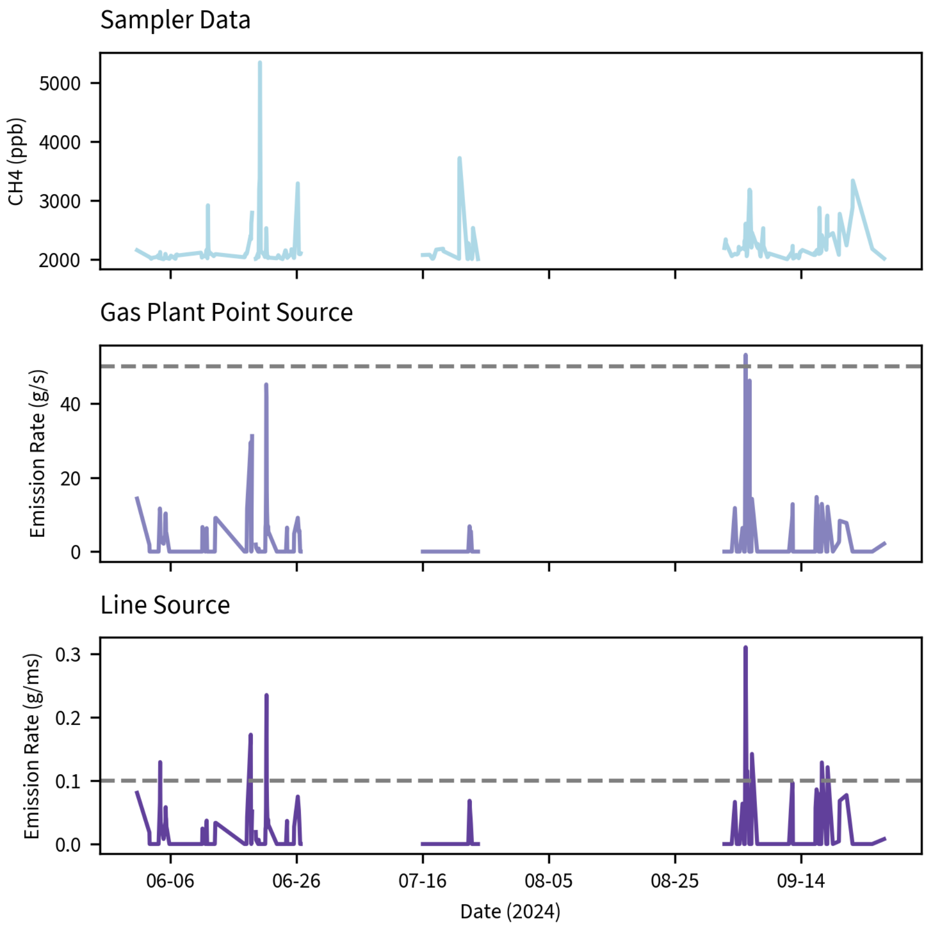

Figure 7: Estimated emissive flux from the landfill site for the line and point sources. Dashed line shows an equal total flux of 50 g s^{-1}

4 Discussion

4.1 Source Geometry

From figure 6, we can evaluate the differences between varying source geometries. It is clear that the LFG plant point source has the best fit, which seems to indicate that the majority of methane comes from the release of LFG after processing. This would agree with ByrneLooby 2022, which indicates that the majority of the site is capped.

Additionally, the constant flux model indicates that the low concentrations are likely to be modelled by a diffuse area source, which agrees with our intuition that the background production of methane will produce a net flux across the site, but that there will be more "spikes" of methane concentration from specific point sources.

The line source also provides a reasonable fit to the data, similar to the area source, while being less computationally intensive.

4.2 Emission Events

In the flux, we find three large spikes in emission. These occur on the 18th June, 21st June, and 5th September. There are a number of explanations for these events. One possibility is landfill collapse events during which trapped bubbles of CH_4 are released. Another is that those dates are when the LFG plant on the site was flaring or leaking gas, releasing excess CH_4.

4.3 Environmental Conditions

We find no strong correlation between our inverted flux the atmospheric parameters in the dataset. Temperature seems to be qualitiatively associated with higher flux (Figure 8), which confirms the findings of Rachor et al. 2013. Higher relative humidity may also be associated with higher source flux, which may be as they are both associated with precipitation. Our data is of limited use for this, and a longer time-scale study should be conducted.

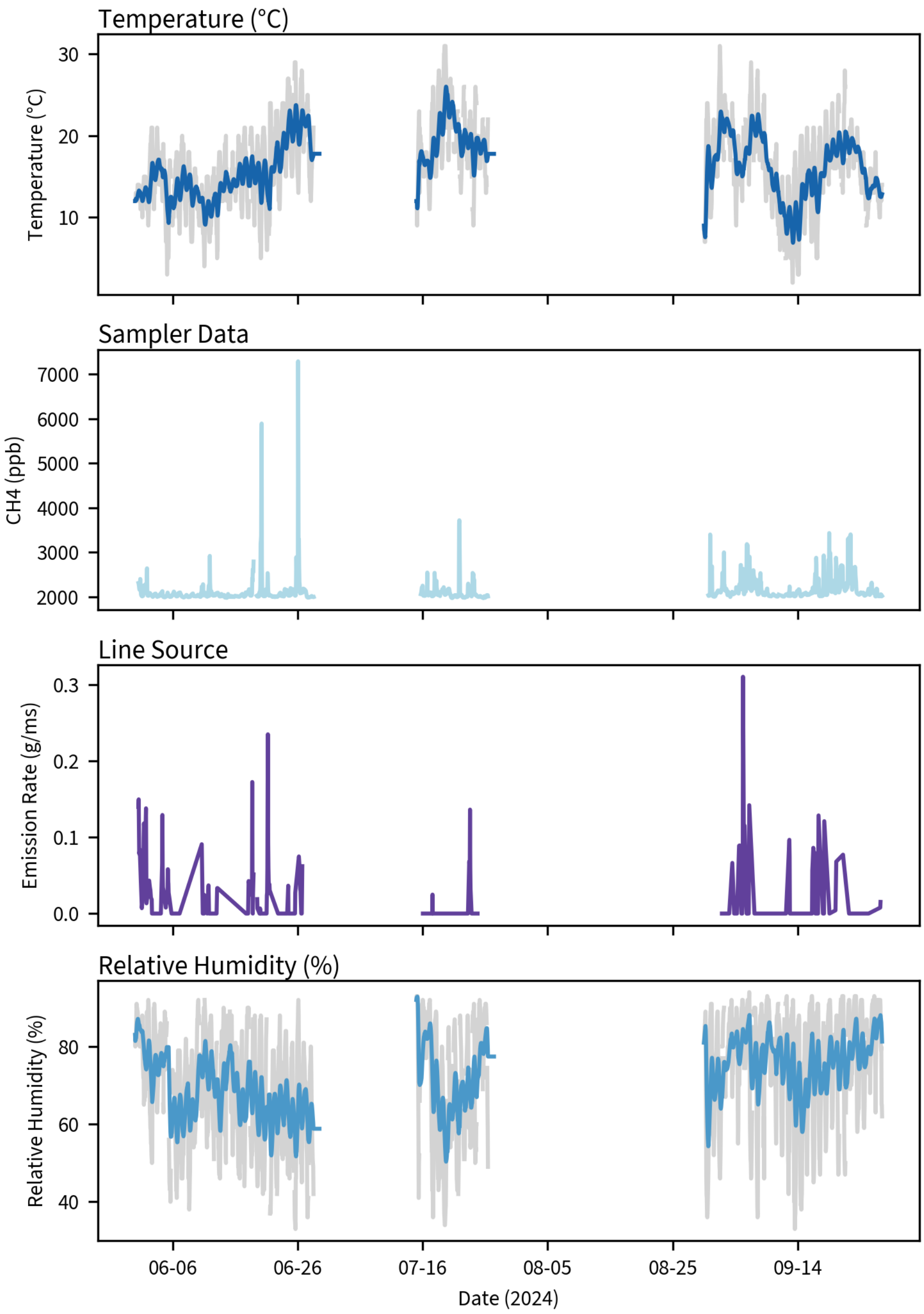

Figure 8: Atmospheric conditions and their effect on the estimated emissive flux.

5 Conclusions

A Gaussian plume model is able to reproduce some of the variation in methane concentration from a landfill source. We find that it is likely that the majority of high methane fluxes come from a point source, roughly located by the LFG treatment plant, whereas the background fluxes are diffuse and perhaps best modelled with an area source.

Sharp emission events punctuate the background flux, which may be associated with landfill collapse events or gas flaring. Temperature and humidity both may contribute to higher source fluxes, though our model cannot quantitatively confirm this.

5.1 Future Work & Improvements

In order to verify the accuracy of this method, chamber and pore fluid measurements could be obtained from the landfill. Specifically, it would be useful to constrain the spatial distribution of emission on active and passive cells, and how that emission varies as a function of time after burial. Having a good spatial dataset would mean we could apply optimisation techniques such as a genetic algorithm or gradient decent to fit a heterogeneous source as was done by Kormi et al. 2018.

Extra data from the landfill records would be helpful; Knowing if there were any gas flare events, leaks in the gas collection or landfill collapse events on June 18th, 21st or Sept 5th would explain the sharp CH_4 peaks. Additional data on cell age and activity would also be welcome.

With that data, it would be possible to model a series of area sources for each cell, with a varying emission based on actual measurements. This would likely give us the best possible model for the contribution from the landfill site. If more information was available about the providence of the dataset (i.e. the instrument used for methane measurements, and its errors), we could better quantify the uncertainty in our model and trends.

Additionally, time dependence could be added to the model by using a Gaussian puff style method (Stockie 2011) with numerical integration (as outlined in appendix B), which would remove the reliance on a short advection time assumption.

References

Beychok, Milton R. (1994). *Fundamentals of Stack Gas Dispersion*. Irvine, CA. : Beychok. URL: https://archive.org/details/fundamentalsofst0000beyc/page/30/mode/2up (visited on 12/09/2024).

ByrneLooby (2022). *Milton Landfill Site Landfill Gas Risk Assessment*. K5348-BLP-R-ENV-00001. FCC Environment UK Limited. URL: https://consult.environment-agency.gov.uk/psc/cb4-6dg-east-waste-limited/supporting_documents/Application%20Variation%2010.%201714%20Milton%20C3%20App%204%20Q6%20LFGRA%2013062022.pdf (visited on 12/09/2024).

Carney, P.G. and V.A. Dodd (1989). "A comparison between predicted and measured values for the dispersion of malodours from slurry". In: *Journal of Agricultural Engineering Research* 44, pp. 67–76. ISSN: 0021-8634. DOI: https://doi.org/10.1016/S0021-8634(89)80071-X. URL: https://www.sciencedirect.com/science/article/pii/S002186348980071X.

CCA (2022). *Global Methane Assessment: 2030 Baseline Report*. Nairobi: United Nations Environment Programme/Climate and Clean Air Coalition.

Delgado, Mónica et al. (2022). "Some findings on the spatial and temporal distribution of methane emissions in landfills". In: *Journal of Cleaner Production* 362, p. 132334. ISSN: 0959-6526. DOI: https://doi.org/10.1016/j.jclepro.2022.132334. URL: https://www.sciencedirect.com/science/article/pii/S0959652622019382.

DESNZ (Feb. 2024). *Final UK greenhouse gas emissions national statistics: 1990 to 2022*. Department for Energy Security and Net Zero. URL: https://www.gov.uk/government/statistics/final-uk-greenhouse-gas-emissions-national-statistics-1990-to-2022 (visited on 12/09/2024).

EA (2010). "Guidance on monitoring landfill gas surface emissions". In: LFTGN07 v2. URL: https://assets.publishing.service.gov.uk/government/uploads/system/uploads/attachment_data/file/321614/LFTGN07.pdf (visited on 12/09/2024).

ECCC (2024). *Methane: keep up the momentum*. Environmental and Climate Change Committee, House of Lords. URL: https://publications.parliament.uk/pa/ld5901/ldselect/ldenvcl/45/45.pdf.

EEA (2023). *Annual European Union greenhouse gas inventory 1990–2021 and inventory report 2023*. European Commission, DG Climate Action, European Environment Agency. URL: https://www.eea.europa.eu/publications/annual-european-union-greenhouse-gas-2.

Fotherby, A. (2024). *QCES methane flux project*. https://github.com/a-fotherby/methane_flux/tree/main/data. (Visited on 12/09/2024).

IPCC (2023). *Climate Change 2023: Synthesis Report.* Contribution of Working Groups I, II, III to the Sixth Assessment Report of the Intergovernmental Panel on Climate Change [Core Writing Team, H. Lee, and J. Romero (eds.)]. IPCC, Geneva, Switzerland, pp. 35–115. DOI: 10.59327/IPCC/AR6-9789291691647.. URL: https://www.ipcc.ch/report/ar6/syr/.

Kissas, K. et al. (2022). "Methane emission dynamics from a Danish landfill: The effect of changes in barometric pressure". In: *Waste Management* 138, pp. 234–242. ISSN: 0956-053X. DOI: https://doi.org/10.1016/j.wasman.2021.11.043. URL: https://www.sciencedirect.com/science/article/pii/S0956053X21006310.

Kormi, Tarek et al. (2018). "Estimation of fugitive landfill methane emissions using surface emission monitoring and Genetic Algorithms optimization". In: *Waste Management* 72, pp. 313–328. ISSN: 0956-053X. DOI: https://doi.org/10.1016/j.wasman.2016.11.024. URL: https://www.sciencedirect.com/science/article/pii/S0956053X16306833.

Lyon, Richard (2012). *Comparative odour potential assessment: Evaluate the impact on odour potential of the changes to the treatment process*. Cambridge WRC. URL: https://www.scambs.gov.uk/media/7201/aw-cambridge-wrc-comparative-odour.pdf (visited on 12/09/2024).

Manheim, Derek C. et al. (2023). "Application of cavity ring-down spectroscopy and a novel near surface Gaussian plume estimation approach to inverse model landfill methane emissions". In: *MethodsX* 10, p. 102048. ISSN: 2215-0161. DOI: https://doi.org/10.1016/j.mex.2023.102048. URL: https://www.sciencedirect.com/science/article/pii/S2215016123000511.

Mønster, Jacob, Peter Kjeldsen, and Charlotte Scheutz (2019). "Methodologies for measuring fugitive methane emissions from landfills – A review". In: *Waste Management* 87, pp. 835–859. ISSN: 0956-053X. DOI: https://doi.org/10.1016/j.wasman.2018.12.047. URL: https://www.sciencedirect.com/science/article/pii/S0956053X18307888.

Nagendra, S.M.S. and Mukesh Khare (2002). "Line source emission modelling". In: *Atmospheric Environment* 36.13, pp. 2083–2098. ISSN: 1352-2310. DOI: https://doi.org/10.1016/S1352-2310(02)00177-2. URL: https://www.sciencedirect.com/science/article/pii/S1352231002001772.

Pasquill, F. (1961). "The estimation of the dispersion of windborne material". In: *The Meteorological Magazine* 90.1063, pp. 33–49.

Rachor, I. M. et al. (2013). "Variability of methane emissions from an old landfill over different timescales". In: *European Journal of Soil Science* 64.1, pp. 16–26. DOI: https://doi.org/10.1111/ejss.12004. eprint: https://bsssjournals.onlinelibrary.wiley.com/doi/pdf/10.1111/ejss.12004. URL: https://bsssjournals.onlinelibrary.wiley.com/doi/abs/10.1111/ejss.12004.

SCRAM, U.S. EPA (Sept. 1995). *User's Guide for the Industrial Source Complex (ISC3) Dispersion Models, Volume II - Description of Model Algorithms*. Tech. rep. EPA-454/B-95-003B. Research Triangle Park, NC: U.S. Environmental Protection Agency. URL: https://gaftp.epa.gov/Air/aqmg/SCRAM/models/other/isc3/isc3v2.pdf.

Smith, R.J. (1993). "Dispersion of Odours From Ground Level Agricultural Sources". In: *Journal of Agricultural Engineering Research* 54.3, pp. 187–200. ISSN: 0021-8634. DOI: https://doi.org/10.1006/jaer.1993.1013. URL: https://www.sciencedirect.com/science/article/pii/S0021863483710139.

Stockie, John M. (2011). "The Mathematics of Atmospheric Dispersion Modeling". In: *SIAM Review* 53.2, pp. 349–372. DOI: 10.1137/10080991X. eprint: https://doi.org/10.1137/10080991X. URL: https://doi.org/10.1137/10080991X.

Sutton, Oliver Graham (1947). "The problem of diffusion in the lower atmosphere". In: *Quarterly Journal of the Royal Meteorological Society* 73, pp. 257–281. URL: https://api.semanticscholar.org/CorpusID:122023956.

T.H. Christensen, R. Cossu and R. Stegmann (2020). *Landfilling of waste. Biogas / edited by T.H. Christensen, R. Cossu, R. Stegmann.* eng. 1st. ISBN: 9781000143898.

Appendices

A Dataset Filtering

In interpreting the dataset, a number of values were found to be outside of a physically explicable range. Therefore there must be some error with calibration or operation of the instruments. Specifically, relative humidity, pressure and wind speed.

A.1 Relative Humidity

Relative humidity was found to be outside of the range 0-100%, which is physically impossible. These values were removed from the dataset. Additionally, a few instantaneous spikes took the values down from over 50 to below 10. I also filtered these.

A.2 Pressure

Negative values were removed from the pressure data.

A.3 Wind Speed

Due to the lack of wind direction data and likely lack of transport, all wind speeds of 0 were removed. Additionally, wind directions were sometimes recorded as 360 (presumably to differentiate from 0), which had to be corrected. Our assumptions require we remove data where the wind speed is recorded as 0, as this means we have no good wind direction data and the wind speed is likely too low for our model to be accurate.

A.4 Wind Direction

We removed data when the sampler is not close to directly downwind of the source, as outside of approximately 30° in each direction from downwind, the model produces extremely high source fluxes. This is likely a sign that the first assumption is breaking down and other local sources are instead contributing CH_4.

B Time Dependent Model

Two approaches can be taken for time dependence. The first, (and simpler), is to simply assume that the concentration forced by a given plume stays in the atmosphere for an exponential decay timescale after the wind stops blowing in that direction. In that case:

$$C(x, y, z, t) = C(x, y, z)e^{-\frac{t}{\tau}} \tag{8}$$

Where τ is the decay timescale, and t is time after wind direction change. This model has limited physical justification, but does give us an estimate for CH_4 removal by reaction and settling.

Mathematically, we can instead derive a "Gaussian Puff" model by providing a solution to the advection-diffusion equation with time dependant boundary conditions with a instantaneous puff of concentration at time 0. This solution can then be integrated or summed numerically. It has the form:

$$C(x, y, z, t) = \frac{Q_T}{8(\pi r)^{3/2}} e^{\left(-\frac{(x-ut)^2+y^2}{4r}\right)} \left[e^{\left(-\frac{(z-H)^2}{4r}\right)} + e^{\left(-\frac{(z+H)^2}{4r}\right)}\right] \tag{9}$$

C Model Dependencies

In producing this report, I defined a new class, `PointSampler`, whose code is available on my Github (removed for anonymity). Additionally, the code to generate area source approximations is available on my GitHub. The dependencies used are listed below:

- `numpy`
- `matplotlib`
- `pandas`
- `scipy`
- `geopy`
- `shapely`
- `windrose`

D Visualisation Motivation

In this section, I justify choices made in the visualisation of the data above. The colour maps, `matplotlib.cm.Purples`, was chosen as monochrome schemes are accessible to the colourblind, and it is visually uniform so will not distort the interpretation of the data.

Figure axes have left large gaps in locations with gaps in the data, which could have been improved by using axes breaks. Unfortunately, matplotlib does not have a robust solution for this. If I had more time, I would treat the datetime objects as text, then index on number and plot a line to indicate an axis break.

The use of the pollution rose in Figure 5 was chosen as it is a common visualisation for pollution concentrations, despite the fact that the plotting of wind speed may have made it unclear.